THESIS

INFLUENCE OF SUBSURFACE HETEROGENEITY ON THE PERFORMANCE OF AQUIFER STORAGE AND RECOVERY IN THE DENVER BASIN

Submitted by

Catharine Cannan

Department of Geosciences

In partial fulfillment of the requirements

For the Degree of Master of Science

Colorado State University

Fort Collins, Colorado

Fall 2016

Master's Committee:

Advisor: Michael Ronayne

Thomas Sale
William Sanford

ABSTRACT

INFLUENCE OF SUBSURFACE HETEROGENEITY ON THE PEROFRMANCE OF AQUIFER STORAGE AND RECOVERY IN THE DENVER BASIN

Aquifer storage and recovery (ASR) is a process through which water is injected into an aquifer for storage and recovered for later use. As water demand worldwide increases there is a growing need to evaluate alternative approaches to water storage, including ASR. Increasing our understanding of the fate of injected water and the subsurface conditions in which ASR is being performed can guide operational choices and decisions on the feasibility of ASR in new regions. Previous evaluations of ASR performance have often assumed homogeneity in the subsurface, overlooking the existence of preferential flow paths created by the combination of transmissive and non-transmissive inter-beds. Because these pathways can influence the lateral transport of water away from injection wells, ASR performance may be impacted. In this study a groundwater flow model within the Denver Basin, Colorado were used to evaluate ASR performance in a heterogeneous subsurface environment. Geologic data in the vicinity of Highlands Ranch, Colorado were synthesized to create heterogeneous, three-dimensional aquifer analogs using multiple-point geostatistical simulation. Flow simulation for these aquifer models was performed to evaluate ASR cycles comprised of injection, storage, and extraction phases, and results were compared to a homogeneous aquifer model. Three metrics were used to assess ASR performance: the extent of hydraulic head changes in the aquifer, fate of injected water particles, and recovery efficiency. Results show that the travel distance of injected water particles was influenced by the presence of heterogeneity and that preferential pathways increase

both the variability and maximum distance traveled by injected water particles. Predicted recovery efficiency decreased slightly when heterogeneity was incorporated, while head change extent was far less sensitive to the presence of heterogeneous structures. These results demonstrate not only the influence of aquifer heterogeneity on ASR performance, but also the potential for geostatistical analysis and numerical modeling to be used as tools for planning future ASR operations.

ACKNOWLEDGEMENTS

I would first like to thank my advisor Michael Ronayne for his guidance and advice throughout the research and thesis writing process. I would also like to express my gratitude to Tom Sale whose expertise, experience, and enthusiasm have been invaluable, and to William Sanford for offering his time to serve on my committee and review my work.

This project was supported by several groups, including the Warner College of Natural Resources' Geosciences Department which presented me with the opportunity to serve as a teaching assistant for three semesters. Colorado State University's Water Center also provided funding for a research assistantship.

Additionally, I would like to thank Centennial Water and Sanitation for the sharing their data and making this study possible. I am specifically grateful to John Kaufman at Centennial and Courtney Hemenway at Hemenway Groundwater Engineering, Inc. for their support and assistance in interpreting the data.

I would like to express my gratitude to Lidstone and Associates (now a Wenck company) for their flexibility and encouragement while I prepared for my defense and for offering me a full-time position through which I can continue to explore my interest in groundwater issues.

Finally, I would like to thank my family and friends for their never wavering support and confidence in me during this remarkable two year journey.

TABLE OF CONTENTS

ABSTRACT ii

ACKNOWLEDGEMENTS iv

LIST OF TABLES vi

LIST OF FIGURES vii

CHAPTER 1: INTRODUCTION 1

CHAPTER 2: HYDROGEOLOGIC SETTING 4

CHAPTER 3: METHODS 9
- 3.1 Data Collection and Interpretation 9
- 3.2 Geologic Cross-Section and Training Image Interpretation 10
- 3.3 Generation of 3-D Aquifer Analogs 11
- 3.4 Numerical Flow Modeling and Particle Tracking 12
- 3.4 ASR Performance Metrics 13

CHAPTER 4: RESULTS 18
- 4.1 Hydraulic Head Change Extent 18
- 4.2 Fate of Injected Water 19
- 4.3 Recovery Efficiency 19

CHAPTER 5: DISCUSSION 24

CHAPTER 6: CONCLUSION AND RECOMMENDATIONS 26
- 5.1 Summary and Conclusions 26
- 5.2 Future Research and Recommendations 27

REFERENCES 29

APPENDIX A 31

LIST OF TABLES

Table 1: Sandstone Fractions Interpreted from Geophysical Data 20

Table 2: Summary of ASR Metrics 21

LIST OF FIGURES

Figure 1: Location and Extent of the Denver Basin Aquifer System 7

Figure 2: Denver Basin Stratigraphic Cross-Section, From Raynolds 2002 8

Figure 3: Interpreted Geophysical Log 15

Figure 4: Cross-Section Location Map 15

Figure 5: Cross-Sections of Subsurface Heterogeneity near Highlands Ranch, CO 16

Figure 6: 3-D Aquifer Analogs 16

Figure 7: Flow Model Domain and Boundary Conditions 17

Figure 8: Simulated Hydraulic Heads after Injection and Storage 21

Figure 9: Extent of Hydraulic Head Change in the Aquifer Following Injection 22

Figure 10: Maximum Particle Travel Extent 22

Figure 11: Minimum Particle Travel Extent 23

Figure 12: Simulated Particle Path Lines 23

CHAPTER 1: INTRODUCTION

Since implementation in the 1960s aquifer storage and recovery (ASR), a process through which water is stored in underground reservoirs during times when demand is low and extracted at a later time when demand increases, has become an important water management strategy (Pyne, 1995). This is particularly true in arid regions and for communities without access to year-round sources of surface water.

In addition to storing potable water, ASR technology has also been used to store treated sewage effluent in areas that require an alternative to surface infrastructure, and to limit the extent of seawater intrusion in coastal regions (Maliva et al., 2011; Misut and Voss, 2007). While ASR can serve as an alternative to storing water in surface reservoirs, it is also used in areas that rely primarily on surface water to increase the resilience of the water supply to natural disasters (Petkewich et al., 2004).

Comparing the effectiveness of ASR under different operational conditions is important for making management decisions. The performance of ASR systems is typically evaluated using a metric known as recovery efficiency, or the percentage of injected water that can be recovered during the extraction phase. Recovery efficiency is mainly of importance in regions where preferential flow paths carry water beyond the capture zone of the ASR wells (Lowry and Anderson, 2006) or where ambient groundwater has higher total dissolved solids (TDS) than injected water, leading to mixing or density driven displacement (Pavelic et al., 2006; Ward et al. 2008). In cases where ambient water is saline or brackish, water quality and the presence of solutes in recovered water is an important indicator of ASR performance (Pavelic et al., 2006; Lowry and Anderson, 2006).

The injection of water causes an increase in hydraulic head within the aquifer which drives lateral flow of water away from the injection well. The induced hydraulic gradient, along with estimated values of hydraulic conductivity and effective porosity, can be used to estimate the travel distance of injected water. However, because the extent of hydraulic head change measures the propagation of energy while the travel distance of water particles is dependent on the processes of advection and diffusion, particle travel and head change propagation distances will differ in an aquifer. In heterogeneous aquifers this discrepancy can be larger and more difficult to predict due to the influence of preferential flow pathways created by the contrasting hydraulic conductivity of geologic units.

A major challenge to the implementation of ASR is the uncertainty in predictions of performance. The influence of a number of operational and hydrogeologic parameters on ASR performance have been studied, including storage time, pumping rates, presence of preferential flow paths, and density of ambient groundwater. However, while it is known that aquifer heterogeneity acts as a control on the accuracy and precision of simulated ASR performance (Pavelic et al., 2006), uncertainty in subsurface structures has meant that the effect of aquifer heterogeneity remains poorly understood. Studies that have considered subsurface heterogeneity have focused on layered aquifer systems, which assume homogeneous aquifers are fully separated by laterally continuous confining layers (Lowry and Anderson, 2006; Ward et al., 2008; Pavelic et al., 2006).

The high cost of subsurface investigations has limited aquifer scale characterization of heterogeneity near ASR well fields and its impact on ASR operation, despite the knowledge that internal geologic architecture exerts a strong control on groundwater flow paths. Further study is needed to investigate how various aspects of ASR system performance are sensitive to aquifer

heterogeneity. Groundwater flow models are particularly useful in this context, allowing for important insights into ASR system sensitivities.

The goal of this paper is to evaluate and compare the performance of ASR in homogeneous and heterogeneous aquifers using multiple metrics, including the extent of head changes, fate of injected water particles, and recovery efficiency. The heterogeneous case was evaluated using a geostatistically simulated aquifer analog that represents the complex hydrogeological conditions of the Denver Basin, Colorado. Pumping rates from the town of Highlands Ranch, CO were used with the goal of realistically modeling the movement of injected water in the subsurface during a period of ASR operation.

CHAPTER 2: HYDROGEOLOGIC SETTING

The Denver Basin is an asymmetric bowl-shaped structure bounded in the west by the Rocky Mountain Front Range of central Colorado (Figure 1). It extends from the Greeley Arch in the north to the Apishapa Arch in the south with no distinct eastern boundary (Raynolds, 2002).

The geologic record of the region reflects the episodic regression of the Western Interior Seaway as well as the growth and subsequent erosion of the Front Range. The basin sediments, formed through the deposition of material eroded from uplifted mountains during the Laramide Orogeny in the late Cretaceous and Tertiary periods, overlie marine shale deposits, left by the Cretaceous Western Interior Seaway, and Pre-Cambrian crystalline igneous and metamorphic rock (Raynolds, 2002; Barkmann et al., 2015). The basement rock begins at the surface near the western edge of the basin and reaches a maximum depth of 4600m near its center. There is a general south-west to north-east trend in the thickness of the basin sediments, with a maximum total thickness of approximately 750 m (Raynolds, 2002).

Groundwater recharge occurs through direct infiltration at limited and discontinuous outcrops along the rim of the basin or through downward flow from overlying leaky aquifers. Outflow in the basin occurs through well extraction or discharge along the South Platte River to the north. With the exception of the deep aquifer formations, where wells are mostly used for industrial or commercial purposes, a majority of the wells in the basin are permitted for domestic or household use.

The Office of the State Engineer of Colorado has characterized, for administrative purposes, four distinct bedrock aquifers that are commonly assumed to be regionally continuous

(Robson, 1987; Paschke, 2011). From oldest to youngest these are the Laramie-Fox Hills, Arapahoe, Denver, and Dawson aquifers.

Recent geologic data suggest that these aquifers are less well defined, and instead are composed of discontinuous sands, siltstones, and shales with limited lateral continuity and internal stratigraphic variability which impacts groundwater flow and availability in the basin (Raynolds, 2002).

This study follows the interpretation of Raynolds (2002) and Raynolds and Johnson (2003), which categorizes the Denver Basin sediments into two distinct depositional pulses, the D1 and D2 sequences, separated by an unconformity (Figure 2). Under this framework stratigraphic units in the basin, from oldest to youngest, are the Pierre Shale, Fox Hills Formation, Laramie Formation, D1 sequence, and D2 sequence (Raynolds and Johnson, 2002). Overlying sediments, including Quaternary sand and gravel deposits, form alluvial aquifers in some regions that generally follow the course of surface streams (Barkmann et al., 2015). This stratigraphic framework is more readily suited towards the incorporation of heterogeneity and the limited lateral extent of aquifer sand layers into considerations of ASR performance.

The Pierre Shale is a dark to light gray, well-bedded marine shale deposited by the Western Interior Seaway during the Cretaceous period (Paschke, 2011). The low-permeability Pierre Shale forms a lower confining unit for the Denver Basin aquifer system. The thickness of this shale layer ranges from approximately 1600 to 2100 meters and the top of the formation, where it transitions gradationally into the Fox Hills Sandstone (Barkmann et al., 2015).

The Fox Hills Sandstone is overlain by and inter-fingers with the shale rich Laramie Formation and is composed of quartz rich sandstone. Both formations were deposited in a coastal plain environment during and after the retreat of the interior seaway. Together, the two

formations are between 150 and 200 meters thick and form the most laterally continuous sandstone aquifer in the basin (Barkmann et al., 2015).

Both the D1 and D2 sequences were deposited by fluvial systems draining the Front Range and are bounded at the top and bottom by unconformities. The D1 sequence is approximately 600 m thick (Barkmann et al., 2015) and was deposited between 68 and 64 Ma (Raynolds and Johnson, 2003). It is lithologically heterogeneous, composed of coarse sandstone, gravel, shale, and mudstone from both granitic and metamorphic sources. In addition to fluvial deposits, paludal deposits and alluvial fan structures are common within the D1 sequence. In general, this sequence is less fine grained than the underlying Laramie and Fox Hills Formations and more heterogeneous than the overlying D2 sequence. Alluvial fan deposits make up the major water producing structures, particularly the Wildcat Mountain Alluvial Fan which includes a majority of the Arapahoe aquifer sandstones in the central part of the basin (Raynolds and Johnson, 2003).

The D2 sequence was deposited approximately 53 to 56 Ma (Raynolds and Johnson, 2003) and is locally separated from overlying sediment by the Wall Mountain ignimbrite, which was deposited during eruptions in the late Eocene. The D2 sequence is approximately 240 meters thick at the center of the basin and has a high ratio of sand to shale and overall higher permeability than the D1 sequence. Because this sequence is nearest to the surface it receives additional recharge from storm water runoff and irrigation return flows (Barkmann et al., 2015).

This paper focuses mainly on the D1 sequence and what are commonly referred to as the Denver and Arapahoe aquifers. Well data used to describe geologic heterogeneity are from Douglas County, CO in the vicinity of Highlands Ranch. Douglas County is part of the rapidly growing South Metro area, a region to the south of Denver that relies on groundwater resources

for municipal supply. Previous work by Barkmann et al. (2011) illustrated how sand bodies in this part of the basin are separated by leaky, laterally discontinuous confining layers and have large amounts of internal heterogeneity.

In 1992 The Centennial Water and Sanitation District (CWSD) began an ASR project in Highlands Ranch, with the goal of supplementing future conjunctive use of both surface water and ground water. Since that time, 19 wells in the region have been used to inject approximately 17 million cubic meters of water into the underlying aquifers. The town continues to operate ASR wells when surface water supplies allow and currently possesses the capacity to inject up to 3 million cubic meters of water per year (CWSD, 2012).

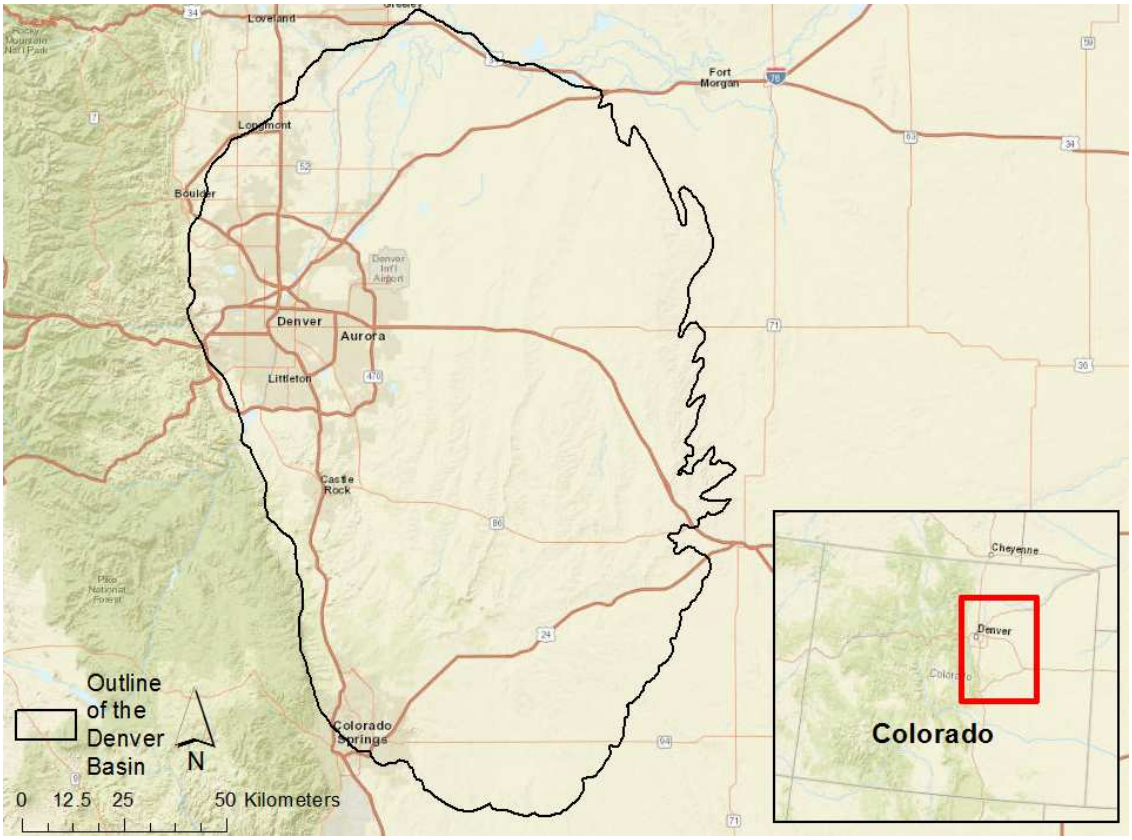

Figure 1: Location and extent of the Denver Basin aquifer system. Denver Basin outline was obtained from Paschke (2011) and coincides with the extent of the Fox Hills sandstone.

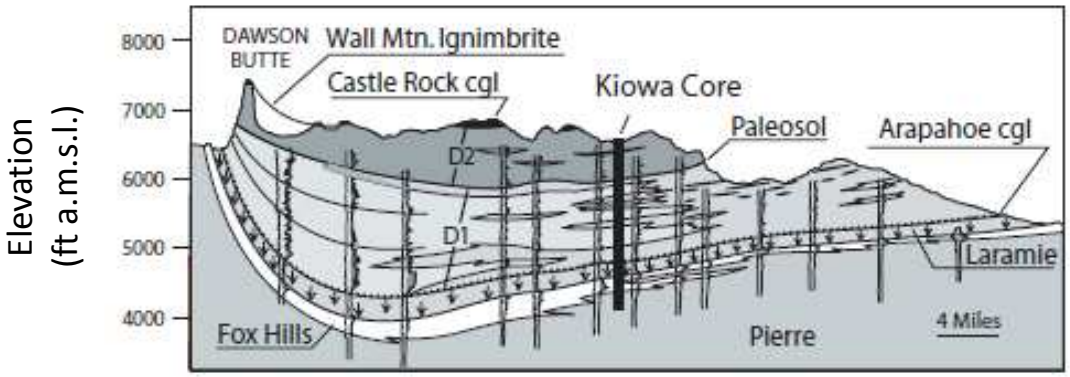

Figure 2: Denver Basin stratigraphic nomenclature as proposed by Raynolds. Figure from (Raynolds, 2002).

CHAPTER 3: METHODS

In order to evaluate the effect of subsurface heterogeneity on ASR performance, synthetic aquifer analogs were constructed using hydrogeologic data from the Highland's Ranch region. These models with heterogeneity were used in flow simulations to evaluate cycles of ASR.

3.1 Data Collection and Interpretation

To characterize the heterogeneity in the region and create representative geologic cross-sections, geophysical well logs in the vicinity of Highlands Ranch were evaluated to identify the position of sandstone and siltstone-shale inter-beds. Geophysical and visual logs for 10 wells were downloaded from the Colorado Division of Water Resources Well Geophysical Log database (CDWR, 2016). Gamma ray, shallow resistivity, and deep resistivity data for each well were converted into digital datasets at a 0.15m (0.5-ft) interval using NeuraLog software (NeuraLog LP., Stafford, TX). The depth to the top of the Arapahoe aquifer was identified at each well from the depths used in the visual log database.

For each of the digitized datasets threshold values corresponding to resistivity and gamma ray shale lines were chosen so that resistivity values above the threshold indicated a sandstone while gamma counts above the threshold indicated a siltstone-shale. Using these thresholds each parameter (shallow and deep resistivity, gamma) was separately labeled as indicative of either sandstone or siltstone-shale within each interval, following the methodology used by previous investigators (Barkmann et al., 2011; Sale et al., 2009).

To account for the varying strengths and weaknesses of each geophysical method, a combination of all three parameters was used to make a lithology call for each depth interval.

Resistivity, the measurement of a formation's capacity to oppose the flow of electricity, is generally high for coarse geologic material and for formation groundwater characterized by low total dissolved solids. Deep resistivity measures formation characteristics farther into the formation than shallow resistivity, which has better resolution for identifying geologic contacts. Gamma ray logs measure radioactive emissions from a formation, which are typically low for the clay poor sandstones of the Denver Basin.

For all depth intervals, the labels assigned using each parameter were compared and lithologic calls made for a given interval when two or more labels agreed (as demonstrated in Figure 3). Using this template the geophysical logs from all 10 wells were transformed into lithologic databases with geologic labels (sandstone or siltstone-shale) applied to each interval continuously throughout the well's extent.

3.2 Geologic Cross-section and Training Image Interpretation

Lithologic cross-sections were generated using Rockware software (RockWare Inc., Golden, Colorado) by importing the location and lithologic calls for each of the 10 wells and allowing the program to interpret lithology between boreholes. Northwest-southeast and southwest-northeast cross-sections were chosen so that each section was composed of 5 wells, the sections were perpendicular to one another, and sections were oriented along or perpendicular to the major axis of the Wildcat Mountain Alluvial Fan, an important depositional structure characterized by abundant coarse-grained material. Cross-section locations are shown in Figure 4.

Between boreholes, lithology was laterally blended to emphasize continuity but also realistic geologic pinch-outs at the farthest extent of each inter-bed. Stratigraphy information

(i.e. aquifer designation) from visual logs was also imported and used to simulate dipping layers within the cross-section. The resulting cross-sections are presented in Figure 5 and are representative of the subsurface heterogeneity in the region.

To facilitate geostatistical modeling, post-processing of the cross-section images was performed using a grid with each pixel assigned a binary number based on its color. Each cross-section was then coarsened in order to create a training image of size 470 x 550 pixels with pixel size 15m x 1m.

3.3 Generation of 3-D Aquifer Analogs

In order to construct three-dimensional aquifer analogs that preserve the interpreted patterns of heterogeneity shown in cross sections, multiple point statistical (MPS) simulation was performed. The s2Dcd program developed by Comunian et al. (2012) was used to generate three-dimensional realizations from two-dimensional training images. The MPS simulations were run using *Impala* (Straubhaar et al., 2011).

The binary versions of the two perpendicular cross-sections (Figure 5) were used as training images, which contain patterns of heterogeneity that will be reproduced in simulated realizations. The s2Dcd program was used to simulate 20 three-dimensional grids (i.e., 20 distinct MPS realizations) of size 250 x 250 x 200 and cell dimensions 15m x 15m x 1m. The s2Dcd program defines a random sequence of two-dimensional surfaces through the domain and for each node along the surface simulates a value representing either sandstone or siltstone-shale, with previously simulated surfaces treated as conditioning data for each sequential step. Because a random simulation path through the grid domain is used, each realization of the s2Dcd program results in a unique aquifer analog, while still preserving the directional patterns of heterogeneity

from the training images. An example of two three-dimensional aquifer analog realizations is shown in Figure 6.

3.4 Numerical Flow Modeling and Particle Tracking

Flow simulations of an operational ASR well were performed using MODFLOW-2000 (Harbaugh et al., 2000). A 120m vertical subset, representing the average thickness of Arapahoe aquifer near Highlands Ranch, was selected from each 3-D aquifer analog realization. Hydraulic conductivities of 0.1m/d or 0.005m/d were assigned to the sandstone and siltstone-shale cells, respectively, which are representative values for these material types in the Denver Basin. In addition to the selected subset of the field with detailed hydraulic conductivity, a buffer zone 20 cells wide was included on each side of the MODFLOW model domain in order to reduce the impact of model boundary conditions on the extent of drawdown and injection cones. Model cells in the buffer zone were assigned a hydraulic conductivity equal to the geometric mean of all the cells within the zone of detailed heterogeneity. The final model grid size was 290x290x120 with cell spacing varying from 141.5 m x 141.5 m x 1 m along the outer edge of the buffer zone to 15 m x 15 m x 1 m within the detailed hydraulic conductivity zone.

The modeled aquifer was treated as confined. A constant hydraulic head boundary was assigned to cells in the top layer of the model along the eastern and western edges to simulate a background regional hydraulic gradient of 0.0018. The upgradient western constant-head value (2437.0 m) and downgradient eastern constant-head value (2428.0 m) were set substantially higher than the layer 1 top elevation (1308.0 m) to simulate a confined aquifer condition. A specific storage of 5.00e-06 m^{-1} was applied to all cells in the model domain. The model domain and boundary conditions are shown in Figure 7.

A single ASR well was modeled at the center of the grid using the revised multi-node well (MNW2) package (Konikow et al., 2009), which allows for the simulation of flow from or into a well open to multiple discrete sandstone inter-beds. This approach allows the total pumping rate to be realistically distributed among the transmissive intervals. A total injection rate of 1067.04 m^3/day and a total pumping rate of -1242.14 m^3/day were chosen as values that represent historic averages at the Highlands Ranch well field. The well was treated as screened for its entire extent.

For each realization, flow simulation was performed to evaluate one cycle of ASR. Three distinct phases in the ASR cycle (injection, storage, and recovery) were implemented using four stress periods. The first stress period represents the steady-state model (with no pumping or injection) and is used to establish initial conditions. Then the ASR cycle was applied over three transient stress periods with ninety days of injection, thirty days of storage (i.e. resting period), and ninety days of recovery. A time step length of one day was used throughout the transient simulation.

In addition to the heterogeneous realizations, a single homogeneous model was created using the same model set-up (i.e. pumping scenarios and boundary conditions) and a single hydraulic conductivity value equal to the geometric mean of the two contrasting conductivities from the heterogeneous realization.

The particle tracking model MODPATH (Pollock, 2012) was used to monitor the movement of injected water. 1920 particles were placed in the model at the beginning of injection, distributed evenly along each of the outward facing edges, in every layer, of the cell that the well passes through. Each particle was tracked forward in time for the entire duration of

the flow simulation; particle tracking step lengths are determined adaptively by the MODPATH code.

3.5 ASR Performance Metrics

In order to assess the impact of aquifer heterogeneity, three metrics were used to quantify ASR performance. For each heterogeneous realization and for the homogeneous aquifer model, the results of flow simulation and particle tracking were recorded and used to calculate the furthest extent of hydraulic head change, the fate of injected water particles, and the recovery efficiency.

The extent of hydraulic head change, or the area of the aquifer affected by the stress of injection, was defined as the distance from the ASR well beyond which there was no hydraulic head change caused by injection. For each realization this was calculated by finding locations within the model domain where simulated drawdown was approximately zero (between -0.1 and 0.1m). Drawdown was calculated as the difference between the simulated head at the end of the second (injection) stress period and the simulated head from the first (steady state) stress period. Locations with zero drawdown were then compared to the coordinates of the ASR well to calculate the radial distance between the points and to identify the model layer in which the maximum head change extent was simulated.

The fate of the injected water was defined as the distance traveled by the injected water particles and their location at the end of injection. For each realization, particle locations at the end of each time step were used to define the travel path of each of the 1920 simulated particles. The location of each particle at the end of the second (injection) stress period was recorded, and

compared to that particle's starting location, to calculate the maximum and minimum radial distance traveled by a particle during each simulation.

Recovery efficiency was defined as the percentage of the injected particles whose ending location, after recovery, was inside the cell that the well passed through. This metric and method of evaluation has been used in previous ASR modeling studies (e.g., Lowry and Anderson, 2006). For each realization the location of all particles at the end of the fourth (recovery) stress period was recorded and compared to the coordinates of the ASR well. If the radial distance between these locations was less than 15m, the width of one model cell, the particle was considered recovered. The sum of recovered particles was used to calculate the recovery efficiency as a percentage of the total number of injected particles.

Depth (m.b.g.s.)	Shallow Resistivity (Ohm-m)	Deep Resistivity (Ohm-m)	Gamma Ray (GAPI)	Label- Shallow Resistivity	Label- Deep Resistivity	Label- Gamma Ray	Geologic Call
139.60	57.50	39.91	162.29	Sand	Sand	Shale	Sandstone
139.75	40.43	27.93	120.19	Sand	Sand	Shale	Sandstone
139.90	20.37	23.89	91.98	Shale	Sand	Sand	Sandstone
140.06	21.00	19.72	91.57	Shale	Sand	Sand	Sandstone
140.21	18.37	14.41	92.50	Shale	Shale	Sand	Siltstone-shale
140.36	15.28	12.30	91.84	Shale	Shale	Sand	Siltstone-shale
140.51	14.87	11.30	101.05	Shale	Shale	Sand	Siltstone-shale
140.67	13.93	9.99	105.93	Shale	Shale	Shale	Siltstone-shale

Figure 3: Subset of interpreted geophysical log of well LFH-11 (location shown in Figure 4) showing the label assigned for each logging method as well as the final geologic call for each depth interval.

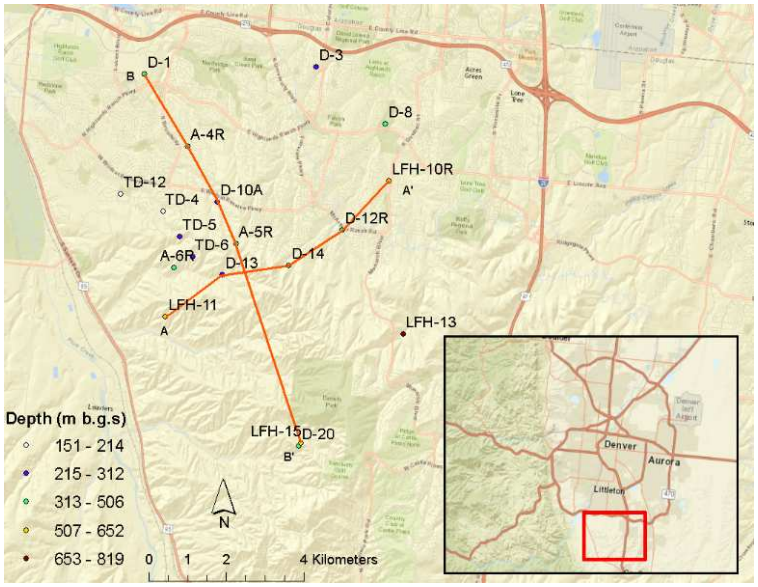

Figure 4: Cross-section location map

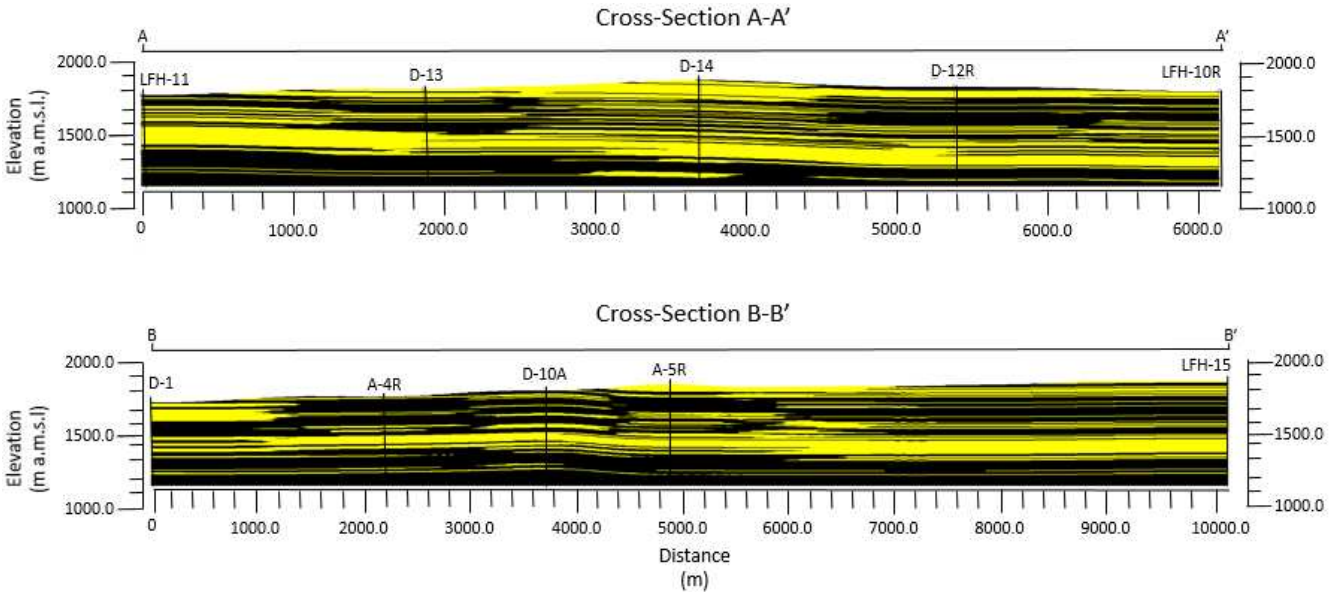

Figure 5: Cross sections representing subsurface heterogeneity near Highlands Ranch, CO. Interpreted sandstone is shown in yellow; black represents siltstone-shale.

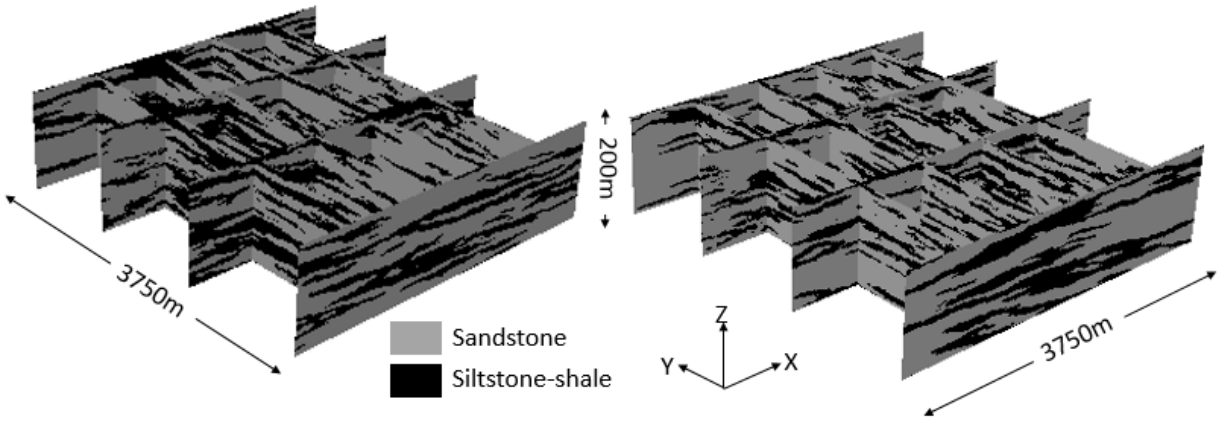

Figure 6: 3-D Aquifer analogs generated using two MPS realizations.

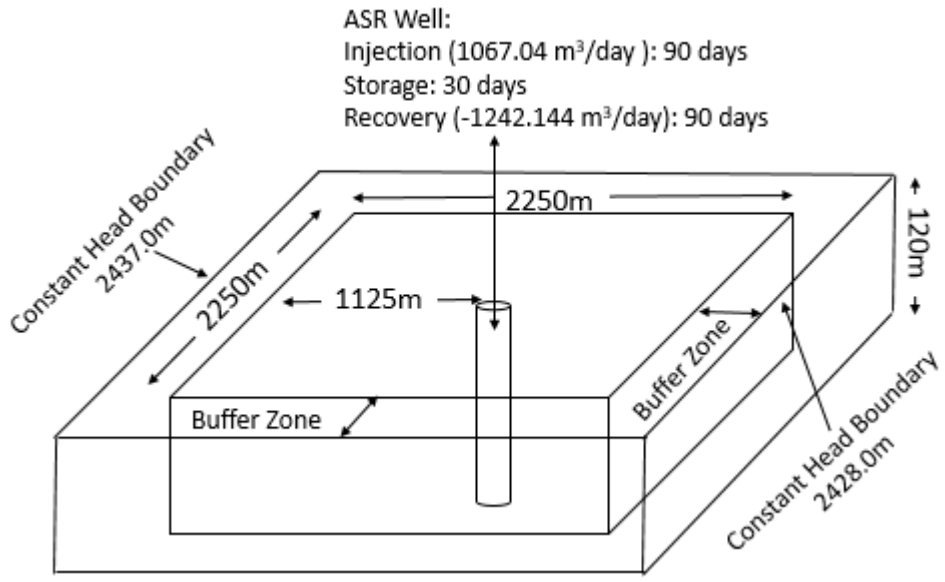

Figure 7: Flow model domain and boundary conditions

CHAPTER 4: RESULTS

Fractions of sandstone and siltstone-shale as determined from the individual geophysical logs are presented in Table 1. The sandstone fraction over the full extent of each log varied between 31% and 56% with an average of 41%. Analysis of the geophysical logs and resulting cross-sections shows that the Arapahoe aquifer in this region is composed of a greater fraction of sandstone than overlying aquifers, with the subset of each log corresponding to the Arapahoe containing between 46% and 80% sandstone. The 3-D aquifer analogs (MPS realizations) contain approximately 61% sandstone and 39% siltstone-shale, which correspond to the fractions present in the two training images (Figure 5).

After conducting flow simulations for twenty realizations of the aquifer heterogeneity (distinct MPS realizations), results converged and the running average for each ASR performance metric changed by less than 0.1% as subsequent realizations were included. Summary statistics from the homogeneous model and twenty heterogeneous realizations are presented in Table 2. Detailed supporting results are included in appendix A.

4.1 Hydraulic Head Change Extent

Simulated hydraulic heads from one realization of the model at the end of injection and storage are shown in Figure 8. The maximum head change in the aquifer occurred at the injection well and ranged between 167.0m at the end of injection to 2.6m at the end of storage.

The maximum extent of hydraulic head change in the aquifer did not differ significantly between the homogeneous model and heterogeneous realizations. For the twenty heterogeneous realizations the average maximum head change extent was 662.4m with a standard deviation of 22.2m. For the homogeneous realization the head change extent was 645.7m. The head change

extent for each realization, in the layer in which the maximum head change extent occurred, is presented in Figure 9.

4.2 Fate of Injected Water

The maximum radial distance traveled by injected water particles was greater, but more variable, for heterogeneous realizations. The radial distance traveled by injected particles in the homogeneous model was 147.3 m, while the maximum distance traveled by injected particles in the heterogeneous realizations averaged 191.5m with a standard deviation of 22.0m. The travel path taken by the particle that traveled the maximum distance in each of the realizations is shown in Figure 10.

The minimum travel distance of injected particles (evaluated after water injection, at the end of stress period 2) was also influenced by the inclusion of heterogeneity. The minimum distance traveled by injected particles in the heterogeneous realizations averaged 31.5m with a standard deviation of 3.6m. This compares to a particle travel distance of 147.3 m in the homogeneous model. The travel path taken by the particle that traveled the minimum distance in each of the realizations is shown in Figure 11.

The individual travel paths of injected particles were influenced by zones of low hydraulic conductivity in the models with heterogeneity. Pathways tended to be tortuous and variable throughout the model domain. Figure 12 shows simulated path lines for particles in two realizations of the heterogeneous model.

4.3 Recovery Efficiency

The inclusion of heterogeneity decreased recovery efficiency. In the homogeneous model 100% of the injected particles were recovered while the average recovery efficiency for the heterogeneous realizations was 97.7% with a standard deviation of 1.5% (Table 2).

Table 1: Percent of geologic material identified as sandstone for each well. Three wells are not deep enough to intersect the Arapahoe aquifer. Fractions are presented for the entire well extent (all depth intervals) and the subset of each log corresponding to the Arapahoe aquifer.

Well Name	Full Well Extent (%)	Arapahoe Aquifer (%)
A-4R	31.1	56.2
A-5R	40.7	65.2
D-1	54.8	45.6
D-10A	33.4	-
D-12R	39.7	45.7
D-13	32.3	-
D-14	56.1	-
LFH-10R	40.4	72.9
LFH-11	41.1	80.1
LFH-15	42.4	69.4
Average	41.2	62.2

Table 2: Summary statistics over 20 realizations of the heterogeneous model for the ASR metrics. Head change extent and particle travel distance were evaluated at the end of the injection phase.

Metric		Heterogeneous Average	Heterogeneous Standard Deviation	Heterogeneous Coefficient of Variation (%)	Homogeneous Case
Hydraulic Head Change	Maximum (m)	662.42	22.24	3.36	-
	Minimum (m)	542.88	13.83	2.55	-
	Average (m)	602.93	9.30	1.54	645.65
Particle Travel Distance	Maximum (m)	191.52	21.98	11.48	-
	Minimum (m)	31.55	3.58	11.35	-
	Average (m)	142.31	6.06	4.26	147.24
Recovery Efficiency		97.65%	1.53%	1.56%	100%

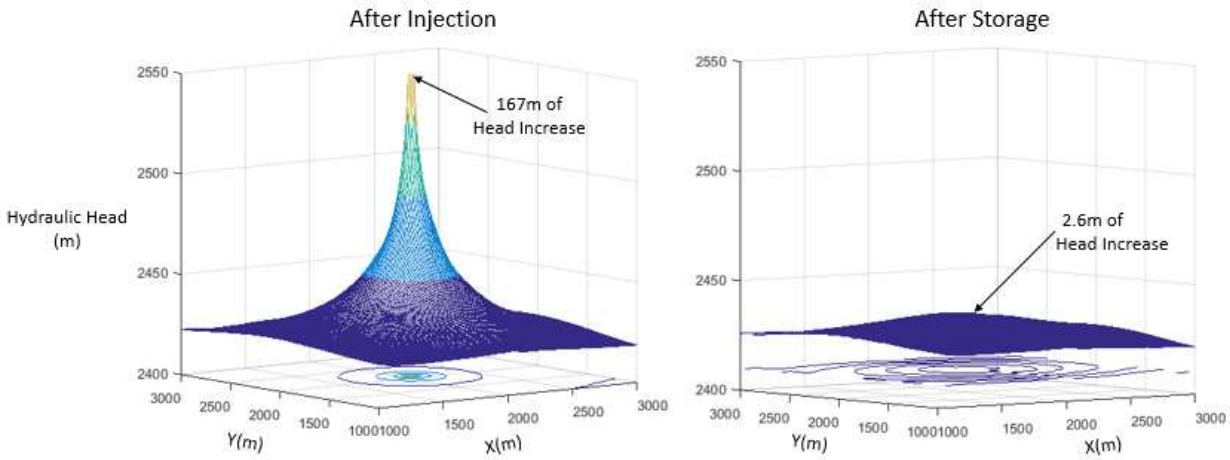

Figure 8: Simulated hydraulic heads in the aquifer immediately following injection and storage phases for one realization of the heterogeneous model. Contours are displayed below surface.

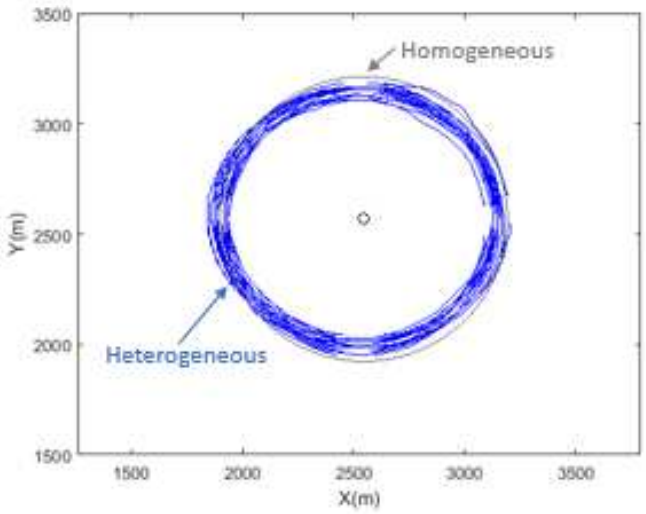

Figure 9: Extent of hydraulic head change in the aquifer caused by injection at the ASR well (black) for each of the heterogeneous realizations (blue) and the homogeneous model (grey). Results are shown for the model layer where the maximum head change extent occurred.

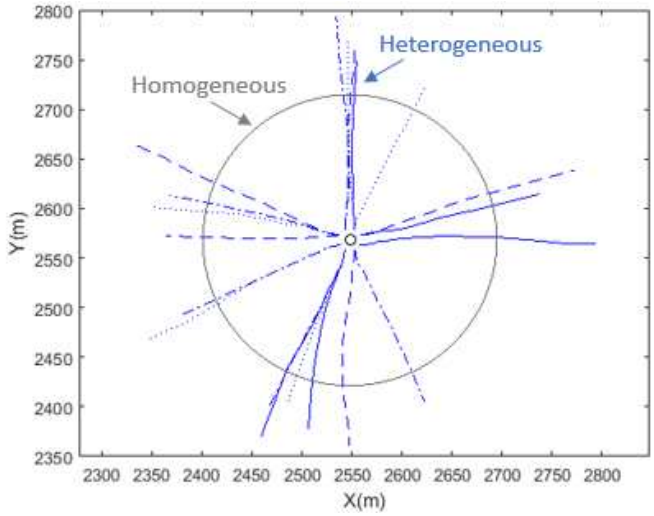

Figure 10: Path lines for particle that traveled the maximum radial distance in each heterogeneous realization (blue) and the travel extent of particles in the homogeneous case (grey). ASR well shown in black.

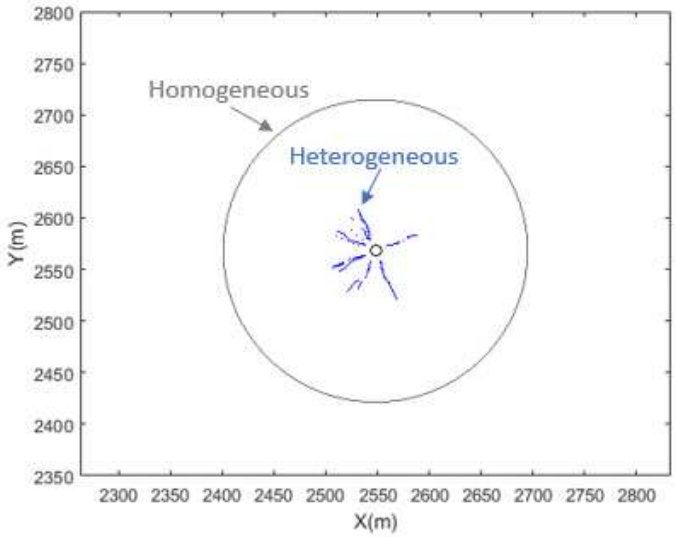

Figure 11: Path lines for particle that traveled the minimum radial distance in each heterogeneous realization (blue) and the travel extent of particles in the homogeneous case (grey). ASR well shown in black.

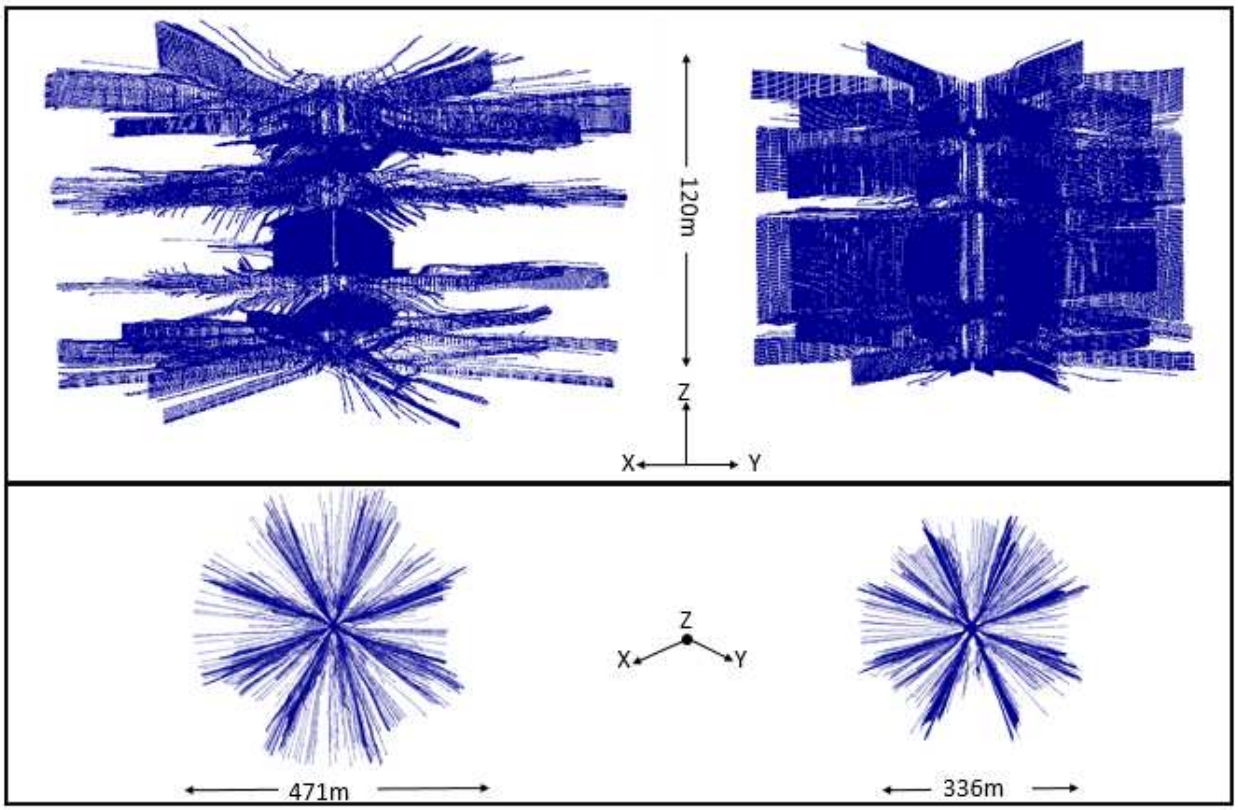

Figure 12: Example of particle path lines from two heterogeneous realizations of the model. Top panel shows cross-sectional view centered on ASR well. Bottom panel provides plan view for each realization.

CHAPTER 5: DISCUSSION

Results of the geostatistical and modeling analysis characterized the heterogeneity of the subsurface in the Denver Basin and the sensitivity of the ASR metrics to the presence of inter-beds with contrasting hydraulic conductivities. The cross-sections and three-dimensional aquifer analogs identified sandstone and siltstone-shale inter-beds in all realizations and illustrate the horizontal connectivity of layers over large distances. While the Arapahoe aquifer in this region contained a higher fraction of sand than overlying zones, no laterally continuous confining layers were identified to support differentiating the sands of the Denver Basin into discrete aquifers.

The presence of subsurface heterogeneity, as modeled for this application in the Denver Basin, does not have a strong impact on the extent of hydraulic head changes in the aquifer. While head change extent in the heterogeneous realizations exhibits some variability (Table 2), in general, ASR operation in heterogeneous and homogeneous subsurface environments impact similar aquifer areas.

Hydraulic head changes caused by injection influenced a larger aquifer area than individual water particle pathways, which demonstrates the difference between the propagation of hydraulic head change and particle travel distance. Differences between head change and particle travel extent will exist in all physical systems and in heterogeneous environments can be larger (Table 2) and more difficult to predict. The need to quantify and compare the two distances supports the use of separate metrics when making predictions related to the effects of ASR.

The impact of preferential pathways created by heterogeneity exerts a strong influence on particle travel distance and a moderate influence on recovery efficiency. Recovery efficiency

decreased in heterogeneous environments because particles could become trapped in low conductivity zones. However, the presence of preferential pathways did not convey water particles beyond the recovery zone for either the homogeneous or heterogeneous cases. Water loss, in the form of injected particles not recovered during extraction, was not significant in the homogeneous or heterogeneous environments and does not act as a barrier to ASR implementation, as long as background water quality is sufficiently high.

The modeling results generated in this study are influenced by the assumption of binary hydraulic conductivities in heterogeneous realizations. By imposing hydraulic conductivity values corresponding to either sandstone or siltstone-shale at every node, heterogeneous realizations were created to represent simplified heterogeneity with sharp hydraulic conductivity contrasts. In reality, the inclusion of different levels of conductivity due to transitional zones or the presence of coarse and fine sandstone fractions will influence predictions of particle travel extents. Also important are the values of hydraulic conductivity assigned to each geologic material. In this study reasonable hydraulic conductivities were used for the sandstone and siltstone-shale, but results at another site where different hydraulic conductivities are used will differ in magnitude. However major results describing the general sensitivity of ASR performance metrics to aquifer heterogeneity are expected to be transferrable to similar hydrogeologic regimes.

CHAPTER 6: CONCLUSION AND RECOMMENDATIONS

5.1 Summary and Conclusions

This thesis investigated the sensitivity of ASR performance to heterogeneity in the subsurface using three metrics: the extent of hydraulic head changes in the aquifer, fate of injected water particles, and recovery efficiency. A method was developed to create three-dimensional aquifer analogs of heterogeneous subsurface environments using multiple-point geostatistical simulation. A groundwater flow model representative of the Denver Basin, CO was used to evaluate performance during one cycle of ASR in order to investigate the sensitivity of each metric to the presence of heterogeneous subsurface structures.

Results support the interpretation of Raynolds and Johnson (Raynolds, 2002; Raynolds and Johnson, 2003) which considers depositional pulses that produced complex heterogeneity in the Denver Basin sediments. The subsurface was characterized as inter-beds of sandstone and siltstone-shale layers with contrasting hydraulic conductivities but without distinct aquifers separated by latterly continuous confining layers. Cross-sections and three-dimensional aquifer analogs were created using limited geophysical information which helps address the high cost of subsurface investigations and the impact of assuming geologic homogeneity when evaluating ASR performance.

The fate of injected water was controlled by the presence of preferential pathways, which influenced both recovery efficiency and travel distance of water particles. Heterogeneity in the subsurface was shown to increase the variability and maximum distance traveled by injected water particles, compared to homogeneous cases, and increase the tendency of injected particles to become trapped in non-transmissive intervals.

Results also exhibit the difference between hydraulic head change extent in the aquifer and travel distance of injected water. While heterogeneity had little impact on head change extent, the fate of injected water was sensitive to the presence of heterogeneous structures in the subsurface. While recovery efficiency and head change extent are commonly used to evaluate ASR performance, our understanding of aquifer response to injection during ASR can be improved by including the fate of injected water as a distinct metric.

While results are sensitive to imposed hydraulic conductivity contrasts and the assumption of binary geologic materials, trends observed in the sensitivity of ASR performance metrics to aquifer heterogeneity and the methods established for characterizing subsurface conditions are expected to be applicable to future investigations in other regions.

5.2 Future Research and Recommendations

Having the necessary tools to evaluate ASR performance can be crucial for investigating the feasibility of ASR in new regions or making management decisions for existing projects. This study demonstrates the impact of ASR in the presence of heterogeneity and supports the need for subsurface characterization when assessing ASR practices. While detailed subsurface investigations can be cost prohibitive, the method presented here supports the use of multiple-point geostatistics and numerical modeling as a supplemental tool that can aid in the characterization of subsurface aquifer properties.

Assumptions that aquifers are vertically discrete and homogeneous can increase uncertainty in predictions of ASR performance and its impact on the aquifer. The geologic characterization performed here does not support differentiating between the Arapahoe, Denver, and Dawson aquifers when evaluating ASR performance metrics. Siltstone-shale inter-beds were identified, which impact the fate and flow path of injected water particles but do not serve

as continuous confining layers. Additional study focused on the identification (or confirmed absence) of confining layers is necessary to better understand the Denver Basin aquifer system.

Of the three metrics used to evaluate ASR performance, the travel distance of injected water particles is the most important to consider in heterogeneous environments when background water quality is sufficiently low in TDS. Recovery efficiency was impacted but may not be a significant restraint to the adoption of ASR in regions with a heterogeneous subsurface, especially in areas with good ambient water quality. The presence of preferential flow pathways in heterogeneous environments should be taken into account in future studies by treating hydraulic head change extent and the fate of injected water as two as separate ASR performance metrics.

Operational parameters used in this study were chosen from ASR well data from Highlands Ranch, CO, but future investigations into the influence of subsurface heterogeneity could be expanded to analyze the impact of operational parameters such as pumping rate and storage time.

Future research could also investigate the performance of ASR in more complex well fields, for example, those with multiple injecting wells or simultaneous injection and extraction occurring at nearby wells. Non-binary lithology could also be used so that geologic intervals are assigned a range of hydraulic conductivity values to account for various compositions.

REFERENCES

Barkmann, P.E., Dechesne, M., Wickham, M.E., Carlson, J., and S. Formolo (2011), Cross sections of the freshwater bearing strata of the Denver Basin between Greeley and Colorado Springs, Colorado, Colorado Geological Survey.

Barkmann, P.E., Fitzgerald, F.S., Sebol, L.A., Curtiss, W., Pike, J., Moore, A., and B. Taylor (2015), Geology and groundwater resources of Douglas County, Open File Report 15-10. Golden, Colorado: Colorado Geological Survey.

Colorado Division of Water Resources (CDWR), 2016. Well geophysical log database. https://data.colorado.gov/Water/DWR-Well-Geophysical-Log/cfyk-gwjj. Accessed Feb 2016.

Centennial Water and Sanitation District (CWSD), 2012. Water Supply Fact Sheet.

Comunian, A., Renard, P., and J. Straubhaar (2012), 3D multiple-point statistics simulation using 2D training images. *Computers & Geosciences*, 40, 49-65.

Harbaugh, A.W., Banta E.R., Hill M.C. and M.G. McDonald (2000), MODFLOW-2000, the U.S. Geological Survey modular ground-water model—user guide to modularization concepts and the ground-water flow process. USGS Open-File Report 00-92. Reston, Virginia: U.S. Geological Survey.

Konikow, L.F., Hornberger, G.Z., Halford, K.J., and R.T. Hanson (2009), Revised multi-node well (MNW2) package for MODFLOW ground-water model: U.S. Geological Survey Techniques and Methods 6-A30.

Lowry, C.S., and M.P. Anderson (2006), An assessment of aquifer storage recovery using ground water flow models. *Ground Water*, 44(5), 661-667.

Maliva, R.G., Missimer, T.M., Winslow, F.P., and R. Herrmann (2011), Aquifer storage and recovery of treated sewage effluent in the Middle East. *Arabian Journal for Science and Engineering*, 36(1), 63-74.

Misut P.E., and C.I. Voss (2007), Freshwater–saltwater transition zone movement during aquifer storage and recovery cycles in Brooklyn and Queens, New York City, USA. *J. Hydrol.* 337:87–103.

Paschke, S.S. ed., (2011), Groundwater availability of the Denver Basin aquifer system, Colorado: U.S. Geological Survey Professional Paper 1770, 274 p.

Pavelic, P., Dillon, P. J., and C. T. Simmons (2006), Multiscale characterization of a heterogeneous aquifer using an ASR operation, *Ground Water*, 44(2), 155-164.

Petkewich, M.D., Parkhurst, D.L., Conlon, K.J., Campbell, B.G., and J.E. Mirecki (2004), Hydrologic and geochemical evaluation of aquifer storage and recovery in the Santee Limestone/Black Mingo aquifer, Charleston, South Carolina, 1998-2002, Scientific Investigations Report 2004-5046. Reston, Virginia: U.S. Geological Survey.

Pollock, D.W. (2012), User guide for MODPATH Version 6—a particle-tracking model for MODFLOW: U.S. Geological Survey Techniques and Methods 6–A41, 58 p.

Pyne, R.D.G. (1995), Aquifer storage recovery: a guide to groundwater recharge through wells. ASR Systems, Gainesville, FL.

Raynolds, R.G. (2002), Upper Cretaceous and Tertiary stratigraphy of the Denver Basin, Colorado, *Rocky Mountain Geology*, 37(2), 111-134.

Raynolds, R.G. and K.R. Johnson (2002), Drilling of the Kiowa Core, Elbert County, Colorado. *Rocky Mountain Geology*, 37(2), 105-109.

Raynolds, R.G. and K.R. Johnson (2003), Synopsis of the stratigraphy and paleontology of the uppermost Cretaceous and lower Tertiary strata in the Denver Basin, Colorado, *Rocky Mountain Geology,* 38(1), 171-181.

Robson, S.G. (1987), Bedrock aquifers in the Denver Basin, Colorado- a quantitative water-resources appraisal: U.S. Geological Survey Professional Paper 1257, 73 p.

Sale, T., Eldiery, A., and A. Bailey (2009), Compilation and Preliminary Analysis of Hydrogeologic Data from the Denver Basin Aquifers in the Vicinity of Castle Rock, Colorado. Colorado State University Report Project Report for the Town of Castle Rock, April 27, 2009.

Straubhaar, J., Renard, P., Mariethoz, G., Froidevaux, R., and O. Besson (2011), An Improved Parallel Multiple-point Algorithm Using a List Approach, *Mathematical Geosciences*, 43(3), 305-328.

Ward, J.D., Simmons, C.T., and P.J. Dillon (2008), Variable-density modelling of multiple-cycle aquifer storage and recovery (ASR): Importance of anisotropy and layered heterogeneity in brackish aquifers, *Journal of Hydrology*, 356(1-2), 93-105.

APPENDIX A

Table A-1: Extent of hydraulic head change- statistical summary for all realizations

Realization	Maximum Extent (m)	Minimum Extent (m)	Average Extent (m)	Standard Deviation (m)	Coefficient of Variation (%)
1	645.17	555.81	602.78	19.66	3.26
2	645.17	555.17	600.01	23.61	3.94
3	712.78	560.04	620.96	46.33	7.46
4	660.17	557.43	601.89	25.49	4.24
5	694.06	547.45	608.01	36.95	6.08
6	662.72	563.85	605.98	23.58	3.89
7	655.21	556.82	598.96	26.21	4.38
8	679.15	541.87	617.19	37.55	6.08
9	638.69	532.66	598.82	22.07	3.69
10	665.77	510.00	588.27	43.89	7.46
11	683.12	540.83	609.79	40.09	6.57
12	653.49	540.83	596.61	26.94	4.52
13	633.03	525.86	589.57	24.59	4.17
14	668.97	540.83	603.31	35.42	5.87
15	668.30	535.39	597.97	34.37	5.75
16	670.32	532.66	604.94	32.39	5.36
17	630.89	541.87	605.02	14.01	2.32
18	691.47	560.04	611.78	35.79	5.85
19	623.89	522.42	582.65	29.46	5.06
20	666.11	537.70	613.99	31.63	5.15
Homogeneous	666.11	632.85	645.65	9.30	1.44

Table A-2: Particle travel distance- statistical summary for all realizations

Realization	Maximum Distance (m)	Minimum Distance (m)	Average Distance (m)	Standard Deviation (m)	Coefficient of Variation (%)
1	235.61	41.69	141.61	74.81	52.83
2	174.31	28.33	144.90	43.59	30.08
3	160.15	28.03	148.66	21.15	14.23
4	178.54	29.49	139.31	55.88	40.12
5	184.49	30.58	143.23	49.65	34.66
6	187.07	29.84	143.82	52.85	36.75
7	191.70	32.85	138.59	63.34	45.70
8	173.51	29.20	140.58	51.08	36.33
9	171.91	29.29	141.82	47.81	33.71
10	226.47	34.73	131.01	79.23	60.48
11	163.61	26.13	146.49	38.62	26.36
12	175.88	28.81	147.62	37.55	25.44
13	206.12	32.80	149.87	59.54	39.73
14	224.77	38.04	129.51	67.95	52.47
15	191.52	31.51	153.88	45.59	29.63
16	217.07	33.37	138.02	70.06	50.76
17	184.70	29.91	146.52	54.22	37.00
18	198.00	32.08	137.23	59.18	43.12
19	216.85	34.65	135.94	70.10	51.56
20	168.21	29.58	147.31	36.94	25.03
Homogeneous	147.34	147.11	147.24	0.07	0.04